ChemComm

Accepted Manuscript

This article can be cited before page numbers have been issued, to do this please use: A. Goswami, S. Pramanik and M. Schmittel, *Chem. Commun.*, 2018, DOI: 10.1039/C8CC01496E.

ROYAL SOCIETY OF CHEMISTRY

rsc.li/chemcomm

View Article Online
DOI: 10.1039/C8CC01496E

ChemComm

COMMUNICATION

Catalytically Active Nanorotor Reversibly Self-Assembled by Chemical Signaling within an Eight-Component Network

xxxxxxxxxxxxxxxxxxxx,
xxxxxxxxxxxxxxxxxxxx

xxxxxxxxxxxxxxxxxxxxxx

www.rsc.org/

Abir Goswami, Susnata Pramanik and Michael Schmittel*

A catalytically active three-component nanorotor is reversibly self-assembled and disassembled by remote control. When zinc(II) ions (2 equiv) are added as an external chemical trigger to the mixture of transmitter $[Cu(\mathbf{1})]^+$ and pre-rotor assembly [(S)•(R)], two equiv of copper(I) ions translocate from $[Cu(\mathbf{1})]^+$ to the two phenanthroline sites of [(S)•(R)]. As a result, $[Zn(\mathbf{1})]^{2+}$ forms along with the three-component assembly $[Cu_2(S)(R)]^{2+}$, which is both a nanorotor (k_{298} = 46 kHz, $\Delta H^{\ddagger}$ = 49.1 ± 0.4 kJ mol^{-1}, $\Delta S^{\ddagger}$ = 9.5 ± 1.7 J mol^{-1} K^{-1}) and a catalyst for click reactions (catalysis ON: A + B →AB). Removal of zinc from the mixture reverts the translocation sequence and thus commands disassembly of the catalytically active rotor (catalysis OFF). The ON/OFF catalytic cycle was run twice in situ in the full network.

The time has come to soar above stand-alone molecular devices[1] and to realize functions[2] in complex supramolecular networks, as ingeniously demonstrated in biological systems.[3] For proper administration of emergent properties in multicomponent ensembles, though, accurate signaling[4] is needed which calls for both selectivity and orthogonality[5] in communication. The high utility of essential metal ions, such as copper(I,II) and iron(II) ions, for cell signaling has become evident recently.[6] Yet, the use of metal ion flux for communication is poorly exploited in (supra)molecular signaling,[7] although it allows selective networking of artificial molecular devices.

Recently, we established a regulated network of two triangular nanoswitches based on copper(I)-ion transfer[8] in response to an external trigger (= iron(II) ions) which enabled ON/OFF control over a catalytic reaction.[8a] In the present work we will demonstrate how self-assembly and disassembly of a catalytically active three-component nanorotor is commanded by chemical communication within an ensemble of eight distinct components. This smart networked nanomachinery allows regulation of both rotational dynamics and catalytic activity through chemical signaling and thus represents an example of advanced molecular cybernetics.

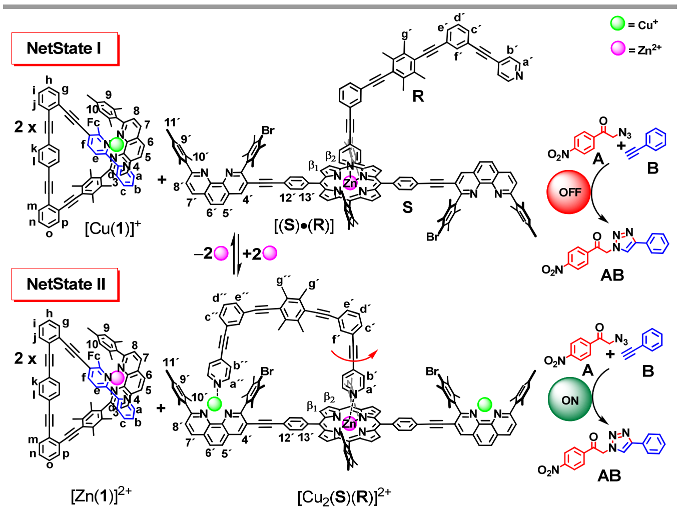

Scheme 1. Cybernetic network between nanoswitch $[Cu(\mathbf{1})]^+$ and nanorotor $[Cu_2(\mathbf{S})(\mathbf{R})]^{2+}$ activated by addition of zinc(II) ions.

The design for the multifunctional cybernetic system in Scheme 1 was based on the following considerations: (1) both the nanoswitch and the nanorotor's components must not interfere with each other in any network state (**NetState**). (2) The metal-ion translocation between nanoswitch and the constituents of the nanorotor should be harmonized in both directions. (3) In the initial self-sorting, the copper(I) ions need to be more weakly bound to the nanorotor's constituents than to the nanoswitch. (4) The nanoswitch must have a higher binding affinity towards the external trigger input so that the liberated copper(I) ions will set up the self-assembled nanorotor and turn ON catalysis. (5) Equally central is the choice of reactants and products in the catalytic reaction, so that there is no interference with the full system.

In response to considerations (1)-(5) we have selected nanoswitch **1**[9] (Scheme 1) because it demonstrated a higher binding affinity (Δlog K = 2.7) toward zinc(II) (ESI[†], Fig. S45)

Center of Micro and Nanochemistry and Engineering, Organische Chemie I, Universität Siegen, Adolf-Reichwein-Str. 2, D-57068 Siegen, Germany
E-mail: schmittel@chemie.uni-siegen.de; Tel: +49(0) 2717404356

Electronic Supplementary Information (ESI) available: Experimental procedures, compound characterizations, spectral data, UV-vis titrations data. See DOI: 10.1039/x0xx00000x than toward copper(I) ions (ESI[†], Fig. S44). Based on recent experience,[10] we came up with a new design for the nanorotor $[Cu_2(\mathbf{S})(\mathbf{R})]^{2+}$. It is based on stator **S**,[11] in which two shielded phenanthrolines (phenAr$_2$) are connected to a zinc porphyrin (ZnPor), and rotator **R** with two identical pyridyl terminals. Both parts are expected to weakly coordinate thus forming the pre-rotor [(**S**)•(**R**)] through pyridine → zinc porphyrin binding ($N_{py} \rightarrow$ ZnPor, log K =3.8).[12] Finally, addition of two equiv of copper(I) ions ought to furnish the three-component nanorotor $[Cu_2(\mathbf{S})(\mathbf{R})]^{2+}$ due to $N_{py} \rightarrow [Cu(phenAr_2)]^+$ binding (= HETPYP[13] binding, log K = 3.2).[10]

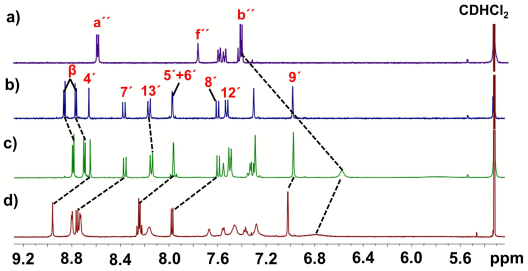

Figure 1. Partial ^{1}H-NMR (400 MHz, CD_2Cl_2, 298 K) of (a) rotator (**R**), (b) stator (**S**), (c) [(**S**)•(**R**)], (d) nanorotor $[Cu_2(\mathbf{S})(\mathbf{R})]^{2+}$.

Preparation of the three-component assembly $[Cu_2(\mathbf{S})(\mathbf{R})]^{2+}$ was readily accomplished by mixing $[Cu(CH_3CN)_4]PF_6$ & ligands **S** and **R** in 2:1:1 ratio in d_2-dichloromethane at 25 °C. The dark violet product is readily characterized by spectroscopic data (^{1}H NMR, ^{1}H-^{1}H COSY, UV-vis, ESI-MS) and elemental analysis. For instance, a single peak at m/z = 1245.1 in the electrospray ionization mass spectrum (ESI-MS) attests the formation of $[Cu_2(\mathbf{S})(\mathbf{R})]^{2+}$ (ESI[†], Fig. S37). In the ^{1}H NMR spectrum of $[Cu_2(\mathbf{S})(\mathbf{R})]^{2+}$ notable downfield shifts of the phenanthroline protons 4´-H, 5´-H, 6´-H, and 7´-H verify the $N_{py} \rightarrow [Cu(phenAr_2)]^+$ complexation whereas upfield shifts of the porphyrin β-H protons indicate the axial $N_{py} \rightarrow$ ZnPor coordination (Figure 1). While stator **S** as a separate molecule displays an absorption at λ = 422 nm, the axial $N_{py} \rightarrow$ ZnPor coordination in [(**S**)•(**R**)] leads to an absorption at λ = 426 nm (ESI[†], Fig. S42). Finally, in $[Cu_2(\mathbf{S})(\mathbf{R})]^{2+}$ the Soret band is located at λ = 429 nm (ESI[†], Fig. S42). A UV-vis titration allowed determination of the overall association constant between **R** and $[Cu_2(\mathbf{S})]^{2+}$ (log K = 7.13 ± 0.28; see ESI[†], Fig. S43). Finally, a single set of ^{1}H-DOSY signals ($D = 3.6 \times 10^{-10}$ m^2 s^{-1}, r ~14.7 Å) proves the clean formation of the assembly (ESI[†], Fig. S30). Importantly, the single set of ^{1}H NMR signals for both phenanthroline units is indicative of a dynamic system. Analogous exchange of dynamic $N_{py} \rightarrow [Cu(phenAr_2)]^+$ interactions was previously seen in speed-regulated four- and five-component nanorotors.[10]

In order to measure the exchange frequency in nanorotor $[Cu_2(\mathbf{S})(\mathbf{R})]^{2+}$, we analyzed the signal (Figure 2) of phenanthroline proton 4´-H that shows up as a sharp singlet (8.96 ppm) at 25 °C in VT ^{1}H NMR studies. Diagnostically, at –60 °C it separates into two singlets (1:1) at 8.93 and 8.89 ppm. The signal at 8.89 ppm corresponds to the pyridine-coordinated phenanthroline station, the freely rotating $[Cu(phenAr_2)]^+$ station furnishes a slightly broader signal at 8.93 ppm (Figure 2). Kinetic analysis provides the exchange frequency (k) at different temperatures (Figure 4a), with k_{298} = 46 kHz (at 298 K). The activation data are $\Delta H^‡$ = 49.1 ± 0.4 kJ mol^{-1}, $\Delta S^‡$ = 9.5 ± 1.7 J mol^{-1} K^{-1} and $\Delta G^‡_{298}$ = 46.6 kJ mol^{-1} (ESI[†], Fig. S32).

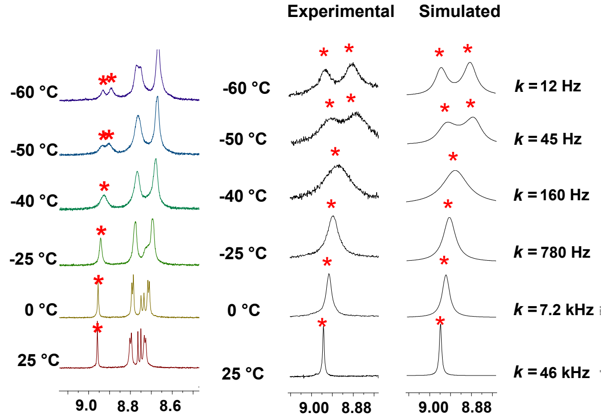

Figure 2. Experimental and theoretical splitting of phenanthroline proton 4´-H of nanorotor $[Cu_2(\mathbf{S})(\mathbf{R})]^{2+}$ in VT ^{1}H-NMR (600 MHz) furnishing rate data in CD_2Cl_2.

For the mechanism of exchange two plausible alternatives may be considered: (i) an intramolecular non-directional rotation requiring the dissociation/association of one $N_{py} \rightarrow [Cu(phenAr_2)]^+$ in the rate-limiting step or (ii) a complete dissociation of $[Cu_2(\mathbf{S})(\mathbf{R})]^{2+}$ into $[Cu_2(\mathbf{S})]^{2+}$ and **R** by cleavage of both the $N_{py} \rightarrow [Cu(phenAr_2)]^+$ and $N_{py} \rightarrow$ ZnPor interactions followed by reassociation. Because full dissociation is endergonic by $\Delta G°_{298}$ = 40.6 kJ mol^{-1} (derived from log K = 7.13), which is smaller than the kinetic barrier of $\Delta G^‡_{298}$ = 46.6 kJ mol^{-1}, the mechanisms cannot be differentiated thereby. However, the kinetic data for exchange in $[Cu_2(\mathbf{S})(\mathbf{R})]^{2+}$ are very similar to those of previously reported nanorotors that operate via a single $N_{py} \rightarrow [Cu(phenAr_2)]^+$ dissociation ($\Delta G^‡_{298}$ = 48.3 kJ mol^{-1}).[14] This good agreement suggests that the exchange mechanism in $[Cu_2(\mathbf{S})(\mathbf{R})]^{2+}$ involves rotation with the $N_{py} \rightarrow$ ZnPor interaction kept intact and the second pyridine terminal of **R** exchanging between the two $[Cu(phenAr_2)]^+$ sites.

For controlling the assembly and disassembly of $[Cu_2(\mathbf{S})(\mathbf{R})]^{2+}$ by metal ion flux through remote control, we decided to test nanoswitch $[Cu(\mathbf{1})]^+$ for its ability to reversibly transmit/receive copper(I) ions to/from the pre-rotor/rotor assembly. The ferrocene and mesityl protons of **1** (Figure 3) serve as diagnostic ^{1}H NMR reporters for metal-ion exchange (copper(I) vs zinc(II) ions).[9] In the ^{1}H NMR of $[Cu(\mathbf{1})]^+$, the ferrocene protons lose their symmetry and shift upfield to 3.32, 3.67, 4.54 and 4.92 ppm in d_2-dichloromethane (ESI[†], Fig. S18). The mesityl protons also shift upfield to 6.35 and 6.43 ppm. In the other switching state, $[Zn(\mathbf{1})]^{2+}$ the ferrocene protons appear at 3.35, 3.84, 4.37, 5.48 ppm and mesityl protons shift to 6.03 and 6.43 ppm in 5:1 CD_2Cl_2:CD_3CN (ESI[†], Fig. S19).

To establish reversible networking between transmitter $[Cu(\mathbf{1})]^+$ and the pre-rotor [(**S**)•(**R**)], we first prepared **NetState I** by mixing **1**, **S**, **R** and $[Cu(CH_3CN)_4]PF_6$ in 2:1:1:2 ratio in d_2-dichloromethane at 25 °C resulting in a dark violet solution. In the ESI-MS a major peak at m/z = 1156.0 (100%) attests the formation of nanoswitch $[Cu(\mathbf{1})]^+$ with its isotopic distribution exactly matching the theoretical one (ESI[†], Fig. S40). Diagnosti-

View Article Online
DOI: 10.1039/C8CC01496D

cally shifted ferrocene and mesityl proton signals in the ^{1}H NMR suggest that the copper(I) ions quantitatively bind to nanoswitch **1** as anticipated (ESI†, Fig. S21). In chorus, the pre-rotor [(**S**)•(**R**)] assembles by intermolecular N_{py} → ZnPor axial coordination, as documented by the Soret band showing up at λ = 426 nm in the UV-vis spectrum (ESI†, Fig. S46).

To generate **NetState II** we added 2.0 equiv of $Zn(OTf)_2$ (as a standard solution in CD_3CN) to **NetState I** at 25 °C. Both, ESI-MS and ^{1}H NMR data (Figure 3b) confirm quantitative formation of $[Zn(\mathbf{1})]^{2+}$ and nanorotor $[Cu_2(\mathbf{S})(\mathbf{R})]^{2+}$. In the ESI-MS we observe a singly charged species at *m/z* = 1307.3 (85%) and a doubly charged one at *m/z* = 578.6 (60%) both reflecting the presence of $[Zn(\mathbf{1})]^{2+}$ after loss of one and two OTf^- counter anions, respectively (ESI†, Fig. S41). Another doubly charged species at *m/z* = 1245.2 (100%) represents $[Cu_2(\mathbf{S})(\mathbf{R})]^{2+}$ (ESI†, Fig. S41). Diagnostic ^{1}H NMR shifts confirm the presence of both complexes $[Cu_2(\mathbf{S})(\mathbf{R})]^{2+}$ and $[Zn(\mathbf{1})]^{2+}$ (ESI†, Fig. S21). Accordingly, addition of zinc(II) ions to **NetState I** has prompted $[Cu(\mathbf{1})]^+$ to deliver copper(I) ions to both empty $phenAr_2$ sites of the pre-rotor. As a result, the free pyridyl terminal of **R** forms a N_{py}→ $[Cu(phenAr_2)]^+$ linkage (HETPYP complex), which finalizes the assembly of nanorotor $[Cu_2(\mathbf{S})(\mathbf{R})]^{2+}$.

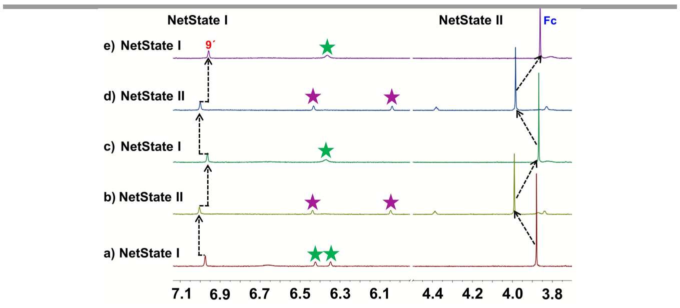

Figure 3. Partial ^{1}H NMR spectra (400 MHz, CD_2Cl_2, 298 K) showing the reversible switching between **NetState I** and **II** over 2.5 cycles. (a) After mixing of $[Cu(CH_3CN)_4]PF_6$, switch **1**, **S**, and **R** in 2:2:1:1 ratio (**NetState I**); (b) after adding 2.0 equiv. of $Zn(OTf)_2$ in CD_3CN furnishing $[Zn(\mathbf{1})]^{2+}$ and $[Cu_2(\mathbf{S})(\mathbf{R})]^{2+}$ (**NetState II**); (c) NMR after addition of 2.0 equiv. of hexacyclen regenerating **NetState I**. Mesityl protons now show up as a broad singlet at 6.36 ppm due to added CD_3CN; (d) addition of 2.0 equiv. of $Zn(OTf)_2$ regenerates **NetState II**; (e) after addition of 2.0 equiv. of hexacyclen.

The kinetics of the copper(I) ion translocation (**NetState I** → **II**) was investigated by UV–vis spectroscopy. Upon addition of 2.0 equiv of $Zn(OTf)_2$, the Soret band absorption shifted instantaneously from λ = 426 to 429 nm (ESI†, Fig. S46). However, ^{1}H NMR analysis indicates that the overall process is not that fast: it takes close to 2 h for complete translocation at 25 °C (Figure 4A). Accordingly, at first the added zinc(II) ions fill the phenanthroline sites of [(**S**)•(**R**)] furnishing $[Zn_2(\mathbf{S})(\mathbf{R})]^{4+}$, which is the cause for the immediate shift of the Soret band. Then in the slow step $[Zn_2(\mathbf{S})(\mathbf{R})]^{4+} + 2\times[Cu(\mathbf{1})]^+ \rightarrow 2\times[Zn(\mathbf{1})]^{2+} + [Cu_2(\mathbf{S})(\mathbf{R})]^{2+}$ the metal ions exchange their positions to furnish the thermodynamically preferred **NetState II** (Figure 4B). To reverse the reaction, we added 2.0 equiv of hexacyclen as a strong chelating agent to **NetState II** at 25 °C. After only 5 min, there was no more diagnostic signal for $[Zn(\mathbf{1})]^{2+}$ left in the ^{1}H NMR and all NMR shifts were fully matching with those of **NetState I** (Figure 3c). Parallel in a UV-vis study, the Soret band shifted immediately from λ = 429 to 426 nm (ESI†, Fig. S46) at 25 °C. Apparently, the hexacyclen first captures the copper(I) ions before exchanging metal ions with switch **1**. Notwithstanding the complex metal ion exchange mechanism, quantitative and reversible switching between **NetState I** and **II** was demonstrated over three cycles (ESI†, Fig. S22).

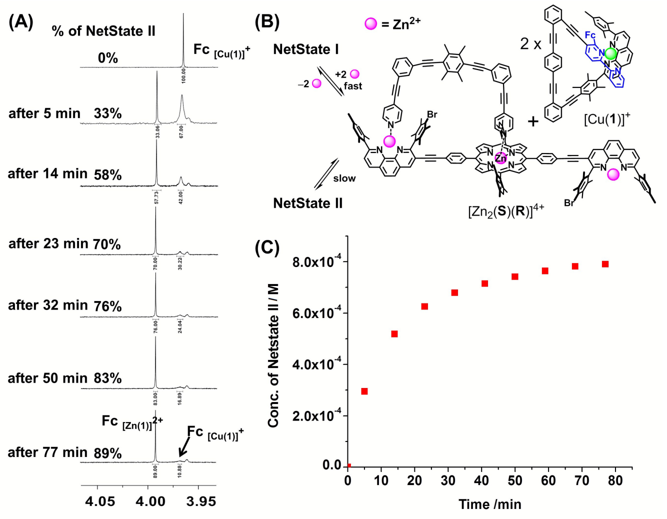

Figure 4. (A) Time dependence of Cu^+ translocation (1.8 mM, CD_2Cl_2, at 298 K) after adding $Zn(OTf)_2$ to a solution of **NetState I**. ^{1}H NMR spectra (400 MHz, CD_2Cl_2:CD_3CN = 5:1) recorded at different times. (B) Intermediate $[Zn_2(\mathbf{S})(\mathbf{R})]^{4+}$ prior to metal exchange. (C) Formation of **NetState II** with time.

Despite the copper(I) ions being dynamically tri-coordinated (HETPYP[13] complexation), the nanorotor $[Cu_2(\mathbf{S})(\mathbf{R})]^{2+}$ (generated in **NetState II**) may have the potential to catalyze a click reaction. In contrast, **NetState I** is expected to shut down any catalysis because Cu^+ is tightly kept in the binding cavity of **1**. To test this hypothesis, a mixture of 2-azido-1-(4-nitrophenyl)ethanone (**A**) and ethynylbenzene (**B**) (1:5) in CD_2Cl_2:CD_3CN = 5:1 was heated at 50 °C for 2 h in presence of 5 mol% of nanorotor $[Cu_2(\mathbf{S})(\mathbf{R})]^{2+}$, furnishing the click product **AB** in (37±1)% yield (ESI†, Fig. S25). A control experiment at identical reaction conditions afforded no product in presence of 10 mol% of nanoswitch $[Cu(\mathbf{1})]^+$ (ESI†, Fig. S26). Equally, free copper(I) ions are not responsible for product formation, because a speciation distribution analysis indicates that only 6% of copper(I) is free in solution and thus <2% of **AB** may arise therefrom (ESI†, Fig. S47). This finding clearly indicates that nanorotor $[Cu_2(\mathbf{S})(\mathbf{R})]^{2+}$ is the active catalyst.

Finally we studied the fully networked catalytic machinery in an ON/OFF manner (ESI†, Fig. S28). For that purpose, **NetState I** was prepared as before and mixed with substrates **A** and **B** in 1: 10 : 50 ratio in d_2-dichloromethane/CD_3CN = 5:1. The mixture was heated for 2 h at 50 °C, but no conversion was detected (Figure 5a,b). Obviously, the copper(I) ions are buried in nanoswitch $[Cu(\mathbf{1})]^+$ (ESI†, Fig. S28) and thus remain catalytically inactive. Now 2.0 equiv of zinc(II) ions were added as a standard solution in acetonitrile-d_3 (75 μL) to generate **NetState II**. The mixture was then heated as before for 2 h at

View Article Online
DOI: 10.1039/C8CC01496E

50 °C and (36±1)% of product **AB** (ESI†, Fig. S28) was detected in ^{1}H NMR (yield from three independent runs). Notably, the catalytic activity of the nanorotor was the same as that of the model reaction in the absence of [Zn(**1**)]$^+$. To turn OFF the reaction, 2.0 equiv of hexacyclen and the consumed amounts of substrates were added to achieve similar reaction condition. After heating for another 2 h using the same conditions, an extra (1.6±0.7)% of product **AB** was detected in ^{1}H NMR. This finding suggests that the copper(I) ions have translocated back to nanoswitch **1** so that they are not available for catalyzing the click reaction. A second cycle furnished similar results (ON: (36±2)%; OFF: 0%) reflecting a remarkable reproducibility of communication and operation within the networked catalytic machinery (ESI†, Fig. S28a,b).

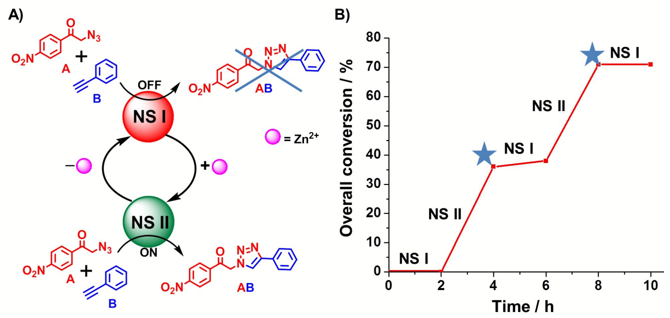

Figure 5. (A) Representation of the ON/OFF regulation of the click reaction in **NetState I** and **II**. (B) Reversible switching between the network states furnishes reproducible amounts of the click product **AB** in **NetState II** (three independent runs). Consumed amounts of substrates were added (blue asterisk).

In conclusion, we have established a multifunctional chemical network of eight components which is able to control both the self-assembly of a three-component nanorotor and its catalytic action. In this multicomponent machinery,[10,15] the addition/removal of zinc(II) ions commands nanoswitch **1** to transmit/receive copper(I) ions that serve as a second messenger. In the forward process, the copper(I) ions assemble a catalytically active three-component nanorotor from a weakly bound precursor complex, in the back process the disassembly leads to a catalytically inactive ensemble. This illustration of molecular cybernetics is a step toward the integral control of different molecular devices[16] operating not any more as individuals but as intricate (supra)molecular machinery. It nicely complements present efforts to run molecular machines using off-equilibrium conditions,[17] so that in the future not only single machines but also networked multi-component machinery may run on chemical fuel.

We thank the DFG (Schm 647/19-2 and 647/20-1) and the University of Siegen for continued support.

Notes and references

(1) (a) M. Schmittel, *Chem. Commun.*, 2015, **51**, 14956-14968; (b) J. C. M. Kistemaker, P. Stacko, J. Visser and B. L. Feringa, *Nat. Chem.*, 2015, **7**, 890-896; (c) M. Xue, Y. Yang, X. Chi, X. Yan and F. Huang, *Chem. Rev.*, 2015, **115**, 7398-7501; (d) A. J. McConnell, C. S. Wood, P. P. Neelakandan and J. R. Nitschke, *Chem. Rev.*, 2015, **115**, 7729-7793; (e) S. Erbas-Cakmak, D. A. Leigh, C. T. McTernan and A. L. Nussbaumer, *Chem. Rev.*, 2015, **115**, 10081-10206.
(2) C. A. Schalley, A. Lützen and M. Albrecht, *Chem. Eur. J.*, 2004, **10**, 1072-1080.
(3) J. Fu, M. Liu, Y. Liu and H. Yan, *Acc. Chem. Res.*, 2012, **45**, 1215-1226.
(4) P. Remón and U. Pischel, *ChemPhysChem.*, 2017, **18**, 1667-1677.
(5) (a) M. L. Saha, S. De, S. Pramanik and M. Schmittel, *Chem. Soc. Rev.*, 2013, **42**, 6860-6909; (b) C.-H. Wong and S. C. Zimmerman, *Chem. Commun.*, 2013, **49**, 1679-1695.
(6) S. C. Dodani, A. Firl, J. Chan, C. I. Nam, A. T. Aron, C. S. Onak, K. M. Ramos-Torres, J. Paek, C. M. Webster, M. B. Feller and C. J. Chang, *Proc. Natl. Acad. Sci. U. S. A.*, 2014, **111**, 16280-16285.
(7) S. Pramanik, S. De and M. Schmittel, *Angew. Chem., Int. Ed.*, 2014, **53**, 4709-4713.
(8) (a) N. Mittal, S. Pramanik, I. Paul, S. De and M. Schmittel, *J. Am. Chem. Soc.*, 2017, **139**, 4270-4273. (b) S. Gaikwad, S. Pramanik, S. De and M. Schmittel, *Dalton Trans*., 2018, **47**, 1786-1790.
(9) S. Pramanik, S. De and M. Schmittel, *Chem. Commun.*, 2014, **50**, 13254-13257.
(10) (a) S. K. Samanta and M. Schmittel, *J. Am. Chem. Soc.*, 2013, **135**, 18794-18797; (b) S. K. Samanta, A. Rana and M. Schmittel, *Angew. Chem., Int. Ed.*, 2016, **55**, 2267-2272.
(11) M. Schmittel, R. S. K. Kishore and J. W. Bats, *Org. Biomol. Chem.*, 2007, **5**, 78-86.
(12) C. H. Kirksey, P. Hambright and C. B. Storm, *Inorg. Chem.*, 1969, **8**, 2141-2144.
(13) HETPYP stands for HETeroleptic PYridine and Phenanthroline complexation: S. Neogi, G. Schnakenburg, Y. Lorenz, M. Engeser and M. Schmittel, *Inorg. Chem.*, 2012, **51**, 10832-10841.
(14) P. K. Biswas, S. Saha, Y. Nanaji, A. Rana and M. Schmittel, *Inorg. Chem.*, 2017, **56**, 6662-6670.
(15) (a) S. Silvi, A. Arduini, A. Pochini, A. Secchi, M. Tomasulo, F. M. Raymo, M. Baroncini and A. Credi, *J. Am. Chem. Soc.*, 2007, **129**, 13378-13379; (b) S. Hiraoka, Y. Hisanaga, M. Shiro and M. Shionoya, *Angew. Chem., Int. Ed.*, 2010, **49**, 1669-1673; (c) Y. Takara, T. Kusamoto, T. Masui, M. Nishikawa, S. Kume and H. Nishihara, *Chem. Commun.*, 2015, **51**, 2896-2898.
(16) G. Ashkenasy, T. M. Hermans, S. Otto and A. F. Taylor, *Chem. Soc. Rev.*, 2017, **46**, 2543-2554.
(17) (a) C. S. Wood, C. Browne, D. M. Wood and J. R. Nitschke, *ACS Cent. Sci.*, 2015, **1**, 504-509; (b) C. Cheng, P. R. McGonigal, S. T. Schneebeli, H. Li, N. A. Vermeulen, C. Ke and J. F. Stoddart, *Nat. Nanotechnol.*, 2015, **10**, 547-553; (c) M. R. Wilson, J. Solà, A. Carlone, S. M. Goldup, N. Lebrasseur and D. A. Leigh, *Nature,* 2016, **534**, 235-240; (d) B. S. L. Collins, J. C. M. Kistemaker, E. Otten and B. L. Feringa, *Nat. Chem.*, 2016, **8**, 860-866; (e) J. A. Berrocal, C. Biagini, L. Mandolini and S. Di Stefano, *Angew. Chem., Int. Ed.*, 2016, **55**, 6997-7001; (f) S. Erbas-Cakmak, S. D. P. Fielden, U. Karaca, D. A. Leigh, C. T. McTernan, D. J. Tetlow and M. R. Wilson, *Science,* 2017, **358**, 340-343. (g) A. Ghosh, I. Paul, M. Adlung, C. Wickleder and M. Schmittel, *Org. Lett*., 2018, **20**, 1046-1049.

View Article Online
DOI: 10.1039/C8CC01496E

Graphical Abstract:

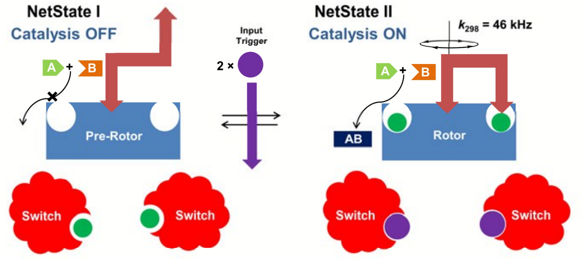

View Article Online
DOI: 10.1039/C8CC01496E

Table of Contents Entry

Catalytically Active Nanorotor Reversibly Self-Assembled by Chemical Signaling within an Eight-Component Network

by Abir Goswami, Susnata Pramanik, Michael Schmittel*

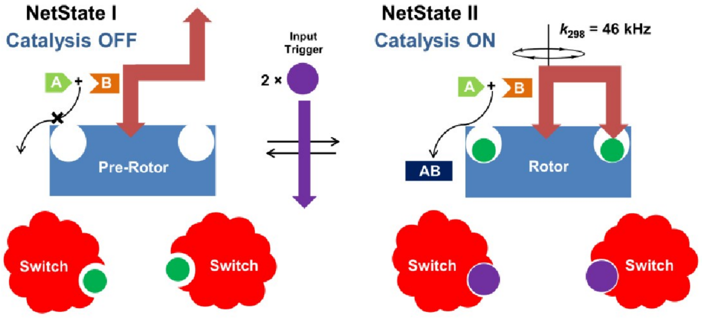

As an example of advanced molecular cybernetics eight components work together through chemical signaling reversibly setting up multifunctional nanomachinery.